Structural Engineering and Mechanics, Vol. 5, No. 5 (1997) 599-608
DOI: http://dx.doi.org/10.12989/sem.1997.5.5.599

Concrete stiffness matrices for membrane elements

Thomas T.C. Hsu†

Department of Civil & Environmental Engineering, University of Houston, Houston, TX, U.S.A.

Abstract. The concrete stiffness matrices of membrane elements used in the finite element analysis of wall-type structures are reviewed and discussed. The behavior of cracked reinforced concrete membrane elements is first described by summarizing the constitutive laws of concrete and steel established for the two softened truss models (the rotating-angle softened-truss model and the fixed-angle softened-truss model). These constitutive laws are then related to the concrete stiffness matrices of the two existing cracking models (the rotating-crack model and the fixed-crack model). In view of the weakness in the existing models, a general model of the matrix is proposed. This general matrix includes two Poisson ratios which are not clearly understood at present. It is proposed that all five material properties in the general matrix should be established by new biaxial tests of panels using proportional loading and strain-control procedures.

Key words: concrete; constitutive laws; cracking; material matrix; membrane element; poisson ratio; reinforced concrete; shear; stiffness; stress-strain relationship.

1. Introduction

1.1. Membrane elements

Large wall-type structures can be visualized as assemblies of two-dimensional membrane elements. The behavior of a whole structure may thus be predicted if the collective behavior of all its component membrane elements can be determined. Finite element analysis is the most powerful method to integrate the load-deformation responses of the component membrane elements (panels) into the load-deformation responses of the whole structure (ASCE 1982, ASCE-ACI 1993).

Cracking in a reinforced concrete membrane element transforms it from a linear, isotropic material into a non-linear, orthotropic material. Being more complex, the behavior of cracked reinforced concrete are not yet clearly understood. Currently, two types of models have been advanced to formulate the post-cracking concrete stiffness matrix for finite element analysis, namely the rotating-crack model and the fixed-crack model. The constitutive laws of concrete and steel for the rotating-crack model are described in the rotating-angle softened-truss model (Belarbi and Hsu 1994, 1995, Pang and Hsu 1995), while those for the fixed-crack model are described in the fixed-angle softened-truss model (Pang and Hsu 1996).

1.2. Fixed-angle vs. rotating-angle

† Professor

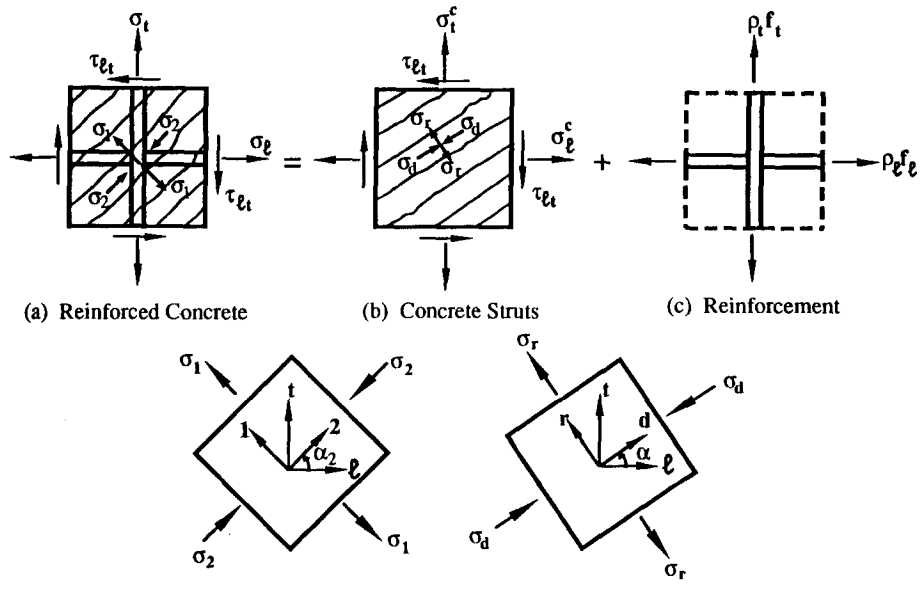

Fig. 1 Coordinate systems and stresses in reinforced concrete membrane elements.

Fig. 1(a) shows a reinforced concrete membrane element subjected to shear and normal stresses. The stresses, τ_{lt}, σ_l and σ_t, are defined in the *l-t* coordinate of the reinforcing steel. The direction of the first batch of cracks is determined by the direction of the principal tensile stresses of the applied stresses. The two principal directions of the applied stresses are defined by the 2-1 coordinate shown in Fig. 1(d). The angle between the 2-1 coordinate and the *l-t* coordinate is called the fixed-angle α_2, because this angle remains constant under proportional loading.

Once the concrete is cracked, the subsequent cracks develop in increasingly divergent directions away from the first crack as a result of changes in the direction of the principal tensile stresses in the concrete, Fig. 1(b). This post-cracking principal direction of concrete depends on the relative amounts of "smeared steel stresses" ($\rho_l f_l$ and $\rho_t f_t$) in the longitudinal and transverse directions, Fig. 1(c), and is defined by the *d-r* coordinate in Fig. 1(e) at any stage of loading. The angle between the *d-r* coordinate and the *l-t* coordinate is called the rotating-angle α, because this angle continues to rotate away from the fixed-angle α_2 under increasing proportional loads. The actual angle of each new crack is observed to lie between α and α_2.

1.3. Softened-truss models

Two types of softened-truss models —rotating-angle softened-truss model and fixed-angle softened-truss model— have been developed to date to predict the behavior of cracked reinforced concrete membrane elements. In the rotating-angle model, the direction of cracks is assumed to orient in the post-cracking principal *d-r* coordinate of concrete at any loading stage. In the fixed-angle model, the direction of cracks is assumed to orient in the principal 2-1 coordinate of the applied stresses. Both these two models satisfy the two-dimensional stress equilibrium, Mohr's circular strain compatibility and the softened biaxial constitutive laws of concrete. They

both can predict the strength as well as the load-deformation history of a membrane element. However, they have two distinct differences: The simpler rotating-angle softened-truss model is unable to predict the "contribution of concrete" (V_c) and has a small range of applicability. The more complex fixed-angle softened-truss model, however, is capable of predicting V_c and has a larger range of applicability (Pang and Hsu 1996, Hsu and Zhang 1997).

2. Constitutive laws of concrete and steel

The key to predicting the behavior of a membrane element by the two softened truss models is the establishment of a set of accurate constitutive laws for concrete and reinforcing bars. These constitutive laws have been determined from full-size (1397×1397×178 mm) reinforced elements using a high capacity and versatile Universal Panel Tester at the University of Houston (Hsu, Belarbi and Pang 1995). The panels were made of concrete with normal strength of 42 MPa (Belarbi and Hsu 1994, 1995, Pang and Hsu 1995, 1996), with medium-high strength of 65 MPa (Zhang 1992), with high strength of 100 MPa (Zhang 1995).

In the finite element method, the concrete and steel bars embedded within concrete can be modeled using the smeared-crack concept. This concept treats cracked concrete as a continuous material. As such, the stresses and strains of concrete and steel in a cracked element are evaluated by averaging (smeared) values. The average stress value between any two adjacent cracks is taken by averaging the stresses occurring between one crack and the midpoint to the adjacent crack. An average strain value is calculated from the displacement measured over a length that traverses several cracks, thus includes the gaps that constitute the cracks.

The average stress-strain relationships of concrete (compression, tension and shear) and mild steel embedded in concrete are proposed for the fixed-angle softened-truss model as follows:

Concrete in compression [Fig. 2(a)]

$$\sigma_2^c=\zeta f_c'\left[2\left(\frac{\varepsilon_2}{\zeta\varepsilon_o}\right)-\left(\frac{\varepsilon_2}{\zeta\varepsilon_o}\right)^2\right] \qquad \frac{\varepsilon_2}{\zeta\varepsilon_o}\le 1 \tag{1a}$$

$$\sigma_2^c=\zeta f_c'\left[1-\left(\frac{\varepsilon_2/\zeta\varepsilon_o-1}{2/\zeta-1}\right)^2\right] \qquad \frac{\varepsilon_2}{\zeta\varepsilon_o}>1 \tag{1b}$$

$$\zeta=\frac{5.8}{\sqrt{f_c'\left(1+\dfrac{400\varepsilon_1}{\eta}\right)}} \quad (f_c' \text{ in MPa}). \tag{2}$$

where σ_2^c is the average compressive stress of concrete in the 2-direction; ε_2 is the average strain in the 2-direction; f_c' is the maximum compressive strength of standard 6 in. by 12 in. (152 mm by 305 mm) concrete cylinder; ε_o is the concrete strain at maximum compressive strength, taken as 0.002 for normal strength concrete of 42 MPa and 0.0024 for the high strength concrete of 100 MPa; ζ is the softening coefficient; and η is a parameter defined as $(\rho_t f_{ty}-\sigma_t)/(\rho_t f_{ty}-\sigma_t)$.

Concrete in tension [Fig. 2(b)]

$$\sigma_1^c=E_c\varepsilon_1 \qquad \varepsilon_1\le 0.00008 \tag{3a}$$

$$\sigma_1^c=f_{cr}\left(\frac{0.00008}{\varepsilon_1}\right)^{0.4} \qquad \varepsilon_1>0.00008 \tag{3b}$$

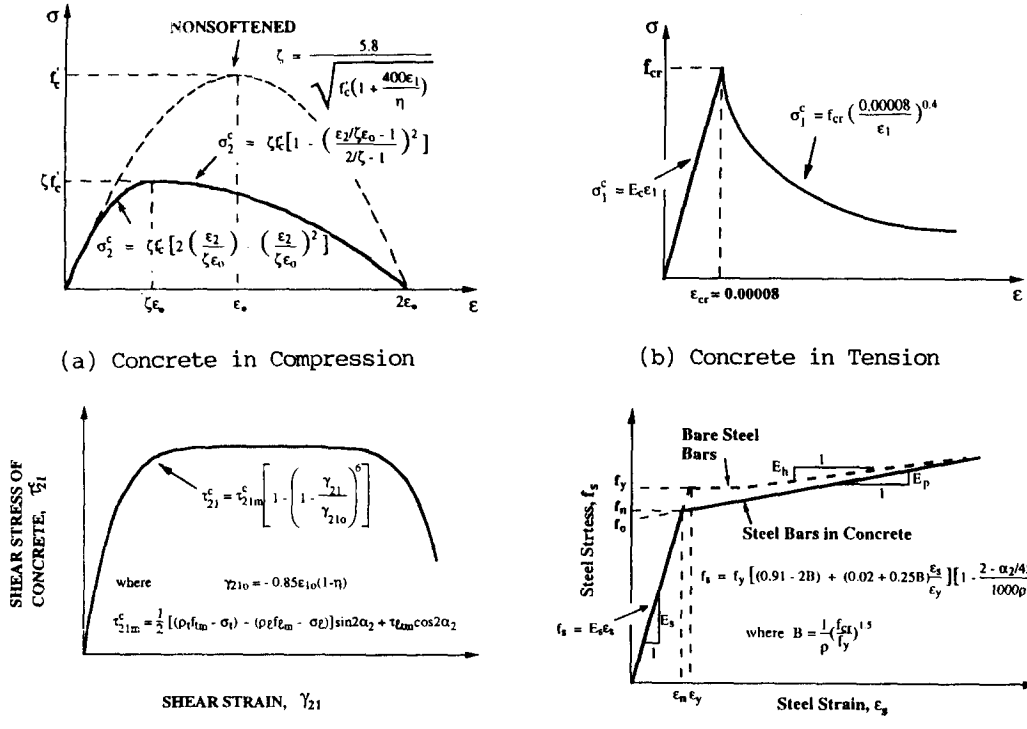

Fig. 2 Average stress-strain curves of concrete and steel in membrane elements.

where σ_1^c is the average tensile stress of concrete in the 1-direction; ε_1 is the average strain in the 1-direction; E_c is the elastic modulus of concrete, taken as 3,875 $\sqrt{f_c'}$; and f_{cr} is the concrete cracking stress, taken as 0.31 $\sqrt{f_c'}$ (f_c' and $\sqrt{f_c'}$ are in MPa).

Concrete in shear [Fig. 2(c)]

$$\tau_{21}{}^c = \tau_{21m}{}^c\left[1-\left(1-\frac{\gamma_{21}}{\gamma_{21o}}\right)^6\right] \tag{4}$$

where
$$\tau_{21m}{}^c = \frac{1}{2}\,[\rho_t f_{tm}-\sigma_t)-(\rho_l f_{lm}-\sigma_l)]\sin 2\alpha_2+\tau_{ltm}\cos 2\alpha_2 \tag{5}$$

and
$$\gamma_{21o} = -0.85\varepsilon_{1o}(1-\eta) \tag{6}$$

where $\tau_{21}{}^c$ is the shear stress of concrete in 2-1 coordinate; γ_{21} is the shear strain of concrete in 2-1 coordinate; $\tau_{21m}{}^c$ is the maximum shear stress of concrete in 2-1 coordinate; γ_{21o} is the shear strain of concrete at maximum shear in 2-1 coordinate; f_{lm} and f_{tm} are average steel stresses at maximum load determined by Eq. (7).

Mild steel [Fig. 2(d)]

$$f_s = E_s\varepsilon_s \qquad \varepsilon_s \le \varepsilon_n \tag{7a}$$

$$f_s = f_y' = f_y\left[(0.91-2\mathrm{B})+(0.02+0.25\mathrm{B})\frac{\varepsilon_s}{\varepsilon_y}\right]\left[1-\frac{2-\alpha_2/45^\circ}{1000\rho}\right] \qquad \varepsilon_s > \varepsilon_n \tag{7b}$$

where ε_n is the average yield strain of mild steel bars embedded in concrete at the beginning

of yielding, defined as $\varepsilon_n=\varepsilon_y(0.93\text{-}2B)\ [1-(2-\alpha_2/45°)/1000\rho]$; f_s is the average stress in mild steel bars and becomes f_l or f_t when applied to longitudinal steel or transverse steel, respectively; ε_s is the average strain in the mild steel bars embedded in concrete and becomes ε_l or ε_t when applied to the longitudinal and transverse steel, respectively; ρ is the reinforcement steel ratio not less than 0.005, and becomes ρ_l or ρ_t when applied to the longitudinal and transverse steel, respectively; α_2 should be between 0 and 90°.

Because the equilibrium and compatibility equations for fixed-angle softened-truss model degenerate into those for the rotating-angle softened-truss model (Hsu 1996), Eqs. (1) to (6) can be simplified when applied to rotating-angle softened-truss model: First, all the subscripts 2 and 1 in the equations should be replaced by d and r, respectively, because the concrete cracks are defined by the d-r coordinate in the rotating-angle model. Second, Eqs. (4) to (6) for concrete in shear become irrelevent, because the shear stress $\tau_{dr}{}^c$ and the shear strain γ_{dr} in the d-r coordinate must vanish. Third, the softened coefficient ζ in Eq. (2) can be simplified by taking $\eta=1$.

3. Models for concrete stiffness

Using the above constitutive laws the concrete stiffness matrices for the two cracking models (rotating-crack model and the fixed-crack model) are determined as follows:

3.1. Rotating-crack model

In this model the cracks are assumed to orient in the principal directions of the concrete (d-r coordinate), and the stress-strain relationships of concrete are:

$$\begin{Bmatrix} \sigma_d \\ \sigma_r \\ \tau_{dr} \end{Bmatrix} = \begin{bmatrix} \bar{E}_d & 0 & 0 \\ 0 & \bar{E}_r & 0 \\ 0 & 0 & \bar{G}_{dr} \end{bmatrix} \begin{Bmatrix} \varepsilon_d \\ \varepsilon_r \\ \gamma_{dr} \end{Bmatrix} \tag{8}$$

The 3×3 matrix represents the cracked concrete stiffness matrix $[D_{dr}]^c$, in which the diagonal elements $\bar{E}_d$ and $\bar{E}_r$ are the secant moduli of concrete in the d- and r-directions, respectively, determined from the constitutive laws in the rotating-angle softened-truss model. In other words, the moduli $\bar{E}_d=\sigma_d/\varepsilon_d$ and $\bar{E}_r=\sigma_r/\varepsilon_r$ are determined from Eqs. (1) to (3), except that the subscripts 2 and 1 in the equations should be replaced by d and r, respectively. The secant shear modulus of concrete $\bar{G}_{dr}=\tau_{dr}{}^c/\gamma_{dr}$, however, is indeterminate, because $\tau_{dr}{}^c=\gamma_{dr}=0$. In practice, therefore, $\bar{G}_{dr}$ is arbitrarily taken as a small value to avoid numerical instability and to fit the overall test results. The value commonly used are $\bar{G}_{dr}=\bar{E}_d\bar{E}_r/(\bar{E}_d+\bar{E}_r)$, or $(\bar{E}_d+\bar{E}_r-2\mu\sqrt{\bar{E}_d\bar{E}_r})/4(1-\mu^2)$, or simply a small fraction of the uncracked shear modulus. Such a practice is theoretically unsound.

3.2. Fixed-crack model

In this model the cracks are assumed to orient in the principal directions of the applied stresses (2-1 coordinate), and the stress-strain relationships of concrete are:

$$\begin{Bmatrix} \sigma_2{}^c \\ \sigma_1{}^c \\ \tau_{21}{}^c \end{Bmatrix} = \begin{bmatrix} \bar{E}_2 & 0 & 0 \\ 0 & \bar{E}_1 & 0 \\ 0 & 0 & \bar{G}_{21} \end{bmatrix} \begin{Bmatrix} \varepsilon_2 \\ \varepsilon_1 \\ \gamma_{21} \end{Bmatrix} \tag{9}$$

The diagonal elements $\overline{E}_2$, $\overline{E}_1$ and $\overline{G}_{21}$ are the secant moduli of concrete in the 2-1 coordinate, determined from the constitutive laws of concrete established experimentally in the fixed-angle softened-truss model. The compressive moduli $\overline{E}_2=\sigma_2^c/\varepsilon_2$ can be determined from the stress-strain curve of concrete in compression given by Eqs. (1) and (2); the tension modulus $\overline{E}_1=\sigma_1^c/\varepsilon_1$ from the stress-strain curve of concrete in tension given by Eq. (3); and the shear modulus $\overline{G}_{21}=\tau_{21}^c/\gamma_{21}$ from the stress-strain curve of concrete in shear given by Eqs. (4) to (6). At present, the modulus $\overline{G}_{21}$ is established from panels with fixed-angle α_2 of 45°, and needs to be checked by panels with fixed-angle from 0 to 90°.

4. A general model

The two softened truss models described above are based on the fundamental assumption that Poisson ratios are zero. This assumption, unfortunately, imposes a limit of application of these models. Pang and Hsu (1995) first discovered that the rotating-angle softened-truss model can predict the load-deformation relationships of membrane elements subjected to shear only if the steel yield stresses, $\rho_l f_{ly}$ and $\rho_t f_{ty}$, in the l- and t-directions satisfy the condition $0.4<\rho_t f_{ty}/\rho_l f_{ly}<2.5$. In other words, when the steel yield stress in one direction is 2.5 times greater than that in the other direction, the model is invalid. In the case of the fixed-angle softened-truss model, Hsu and Zhang (1997) found a wider range of applicability of $0.2<\rho_t f_{ty}/\rho_l f_{ly}<5$. In both cases, the limits of application are rooted in the assumption that Poisson ratios are zero, and these limits can be removed only if the Poisson ratios are taken into account in the analysis.

4.1. Proposed concrete stiffness matrix

This paper proposes a general model which includes two Poisson ratios in the analysis. The concrete stiffness matrix, defined in the principal 2-1 coordinate and including the Poisson ratios, can be written as follows:

$$[D_{21}]^c=\begin{bmatrix} \overline{E}_2 & \nu_{12}\overline{E}_2 & 0 \\ \nu_{21}\overline{E}_1 & \overline{E}_1 & 0 \\ 0 & 0 & \overline{G}_{21} \end{bmatrix} \tag{10}$$

where ν_{12} is the tension-compression Poisson ratio and ν_{21} is the compression-tension Poisson ratio. Eq. (10) is the most general form of material stiffness matrix in a two-dimensional, orthogonal model, when the coordinate of principal tensile strains is assumed to coincide with the coordinate of principal tensile stresses.

4.2. Poisson ratios

In order to measure the two Poisson ratios, reinforced concrete membrane elements (or panel) with $\alpha_2=90°$ were tested biaxially under sequential loading by Zhang and Hsu (Zhang 1995, Hsu, Zhang and Gomez 1995). These tests showed that the tension-compression Poisson ratio ν_{12} is $-10\rho_1/(2+1000\varepsilon_1)$, where ρ_1 and ε_1 are the steel ratio and tensile strain, respectively, in the principal 1-direction; while the compression-tension Poisson ratio ν_{21} is 0.62. Both the negative value of ν_{12} and the value of ν_{21} greater than 0.5 are rather surprising, because they can not

occur in a continuous material. These values can be explained, however, by the slippage and wedging actions between the concrete and the deformed steel bars in a cracked, discontinuous reinforced concrete material.

The values of tension-compression Poisson ratio ν_{12} obtained by Vecchio and DeRoo (1995) was in the order of -0.03 to -0.16. These values are greatly exaggerated, because they were obtained from tests controlled by tensile load in one direction and zero load in the perpendicular direction. In these uniaxial, load-control tests, each perpendicular strain measurement contains two parts. While one part is caused by real deformation of the material, the other part is not a true component but one caused by the air gaps that constitute the cracks. The value of Poisson ratio ν_{12} obtained by Zhang and Hsu was carried out in biaxial, strain-control tests using a servo-control system. This ν_{12} value reflects only the strain that corresponds to a real stress, and not the air gaps that can be closed by almost no stress.

Even with the biaxial, strain-control tests, it is doubtful that the two Poisson ratios obtained by Zhang and Hsu can be applied in Eq. (10). First, the panels used by Zhang and Hsu are reinforced with longitudinal steel in the direction of the principal tensile stress (α_2 of 90°). It is not clear whether the two Poisson ratios so obtained are applicable to panels with reinforcing steel in an arbitrary direction (α_2 from 0° to 90°). Second, the ratios ν_{12} and ν_{21} were determined from sequential loading, a load path that differs from the proportional loading that is used to determine the moduli $\bar{E}_2$, $\bar{E}_1$ and $\bar{G}_{21}$ in Eq. (10). Garza's recent tests (1996) showed, however, that load path has a strong effect on the stress-strain surface of concrete. As such, these two Poisson ratios are unlikely to be consistent with the three moduli obtained from proportional loading.

A consistent set of five mechanical properties ($\bar{E}_2$, $\bar{E}_1$, $\bar{G}_{21}$, ν_{12} and ν_{21}) in Eq. (10) should be established by extensive new experiments where panels with various steel angles are subjected to the same proportional loading.

4.3. Proposed tests

The panel tests will be carried out by strain-control mode using the servo-control system (Hsu, Zhang and Gomez, 1995). In addition to the Poisson ratios, the strain-control mode also allows us to measure the descending branches of the stress-strain curves of concrete in compression, tension and shear.

Panels with steel bars in four different orientations (α_2=90°, 68.2°, 45°, and 21.8°) will each be subjected to a principal tensile stress σ_1 and a principal compressive stress σ_2 of equal magnitude ($\sigma_2=-\sigma_1$), Fig. 3. They will be both increased in a proportional manner along a 45° dotted line as shown in Fig. 4(a), so that a pure shear stress is created at an angle of 45° to the principal 2-1 coordinate.

The proportional loading is approximated by small step-wise increases as shown in Fig. 4(a) so that Poisson ratios can be measured at each load stage. At low loads, the stress-control mode will be used to apply σ_1 and σ_2. When σ_1 is increased, say, from point 2 to point 3, σ_2 is maintained constant. The ratio of the increment of strain ε_2 (Fig. 4(c)) to the increment of strain ε_1 (Fig. 4(b)) from point 2 to point 3 represents the tension-compression Poisson ratio ν_{12}. When σ_2 is increased, say, from point 3 to point 4, σ_1 is maintained constant. The ratio of the increment of strain ε_1 (Fig. 4(b)) to the increment of strain ε_2 (Fig. 4(c)) from point 3 to point 4 represents the compression-tension Poisson ratio ν_{21}.

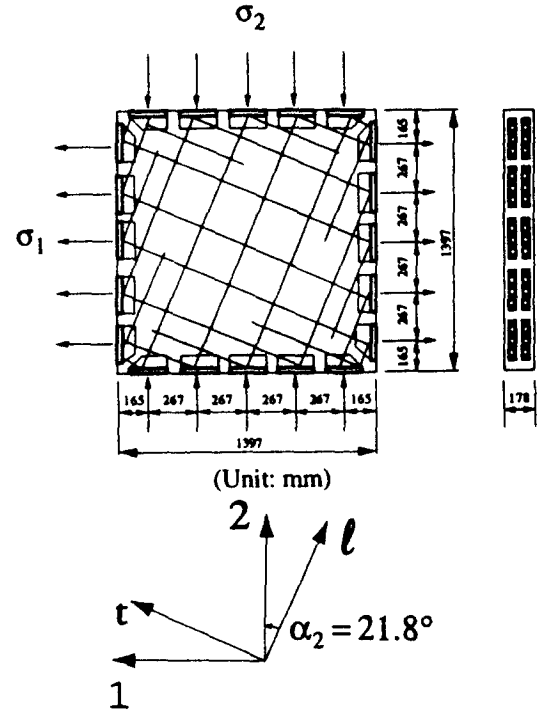

Fig. 3 A typical test panel.

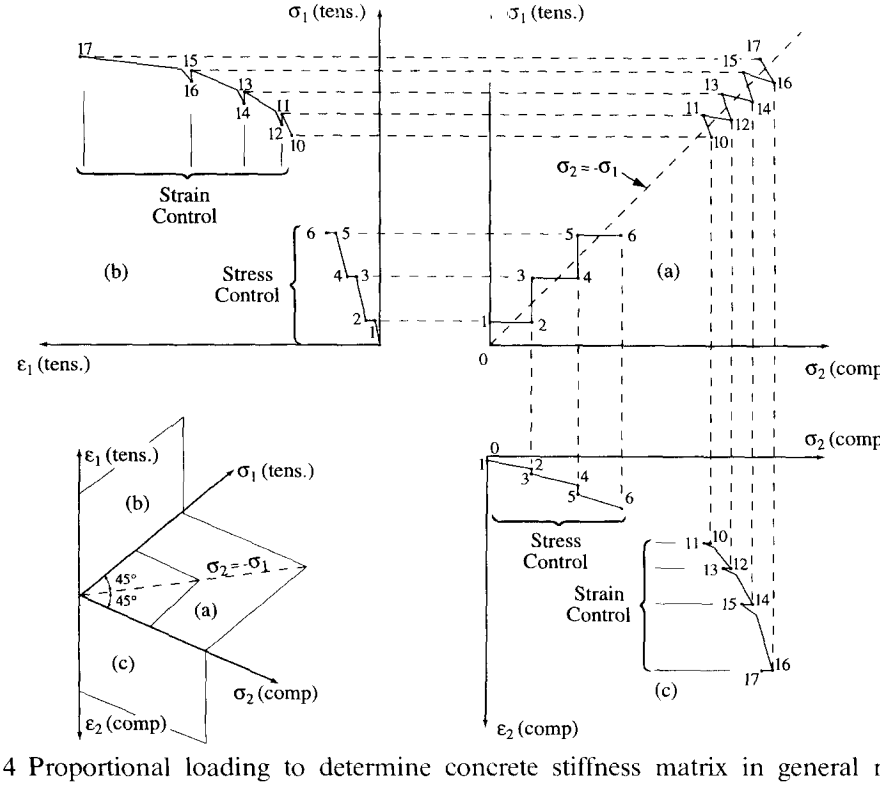

Fig. 4 Proportional loading to determine concrete stiffness matrix in general model.

At high loads after the yielding of steel, a small increase of load will produce a large increment of strain. This large increment of strain becomes uncontrollable when the maximum load is approached, thus resulting in a sudden failure without obtaining the descending branch of the load-deformation curve. Therefore, strain-control mode must be used at the high load stages to control both ε_1 and ε_2. When ε_1 is increased, say, from point 14 to point 15 (Fig. 4(b)), ε_2 is maintained constant (Fig. 4(c)). The decrement of strain ε_2 required by the Poisson ratio ν_{12} will then be calculated from the drop of the stress σ_2 from point 14 to point 15 using the unloading stiffness in the 2-direction. Similarly, when ε_2 is increased, say, from point 15 to point 16 (Fig. 4(c)), ε_1 is maintained constant (Fig. 4(b)). The decrement of strain ε_1 required by the Poisson ratio ν_{21} will then be calculated from the drop of the stress σ_1 from point 15 to point 16 using the unloading stiffness in the 1-direction.

By subtracting the effect of reinforcement from the stress-strain relationships (σ_2 vs. ε_2 and σ_1 vs. ε_1) shown in Fig. 4(b) and (c), the compressive and tensile stress-strain curves of concrete [σ_2^c vs. ε_2 and σ_1^c vs. ε_1] can be calculated, from which the two moduli $\overline{E}_2$ and $\overline{E}_1$ are determined. By measuring the additional strains ε_l and ε_t in the *l-t* coordinate, the shear stress-strain curves of concrete [τ_{21}^c vs. γ_{21}] can be calculated, from which the shear modulus $\overline{G}_{21}$ is determined. These three moduli $\overline{E}_2$, $\overline{E}_1$, and $\overline{G}_{21}$ will be consistent with the two measured Poisson ratios ν_{12} and ν_{21}, because they are all obtained under the same proportional loading.

5. Application in finite element analysis

Assuming that the *l-t* coordinate of reinforcement is the global coordinates, the concrete stiffness matrix $[D_{21}]^c$ in the 2-1 coordinate, Eq. (10), can be transformed to the concrete stiffness matrix $[D]^c$ in the *l-t* coordinate (global coordinate):

$$[D]^c=[T]^T\ [D_{21}]^c[T] \tag{11}$$

The transformation matrix $[T]$ is given by:

$$[T]=\begin{bmatrix} \cos^2\alpha_2 & \sin^2\alpha_2 & -\sin\alpha_2\cos\alpha_2 \\ \sin^2\alpha_2 & \cos^2\alpha_2 & \sin\alpha_2\cos\alpha_2 \\ 2\sin\alpha_2\cos\alpha_2 & -2\sin\alpha_2\cos\alpha_2 & (\cos^2\alpha_2-\sin^2\alpha_2) \end{bmatrix} \tag{12}$$

Using the smeared steel stresses, $\rho_l f_l$ and $\rho_t f_t$, the reinforcement stiffness matrix $[D]^s$ in the *l-t* coordinates is evaluated as

$$[D]^s=\begin{bmatrix} \rho_l\overline{E}_l & 0 & 0 \\ 0 & \rho_t\overline{E}_t & 0 \\ 0 & 0 & 0 \end{bmatrix} \tag{13}$$

where $\overline{E}_l$ and $\overline{E}_t$ are the secant moduli of steel bars in the *l*- and *t*-directions, respectively. $\overline{E}_l=f_l/\varepsilon_l$ and $\overline{E}_t=f_t/\varepsilon_t$ are determined from the stress-strain curve of steel embedded in concrete given by Eq. (7).

The total material stiffness matrix is the summation of the concrete stiffness matrix and the reinforcement stiffness matrix in the global coordinate system as

$$[D]=[D]^c+[D]^s \tag{14}$$

Then the smeared stress-strain relationship of an element in the *l-t* coordinates can be expressed

as

$$\begin{Bmatrix} \sigma_l \\ \sigma_t \\ \tau_{lt} \end{Bmatrix} = [D] \begin{Bmatrix} \varepsilon_l \\ \varepsilon_t \\ \gamma_{lt} \end{Bmatrix} \tag{15}$$

Eq. (15) can be implemented into the smeared-crack model of finite element analysis.

Acknowledgements

The preparation of this paper is partially supported by the National Science Foundation Grant No. CMS-9213707.

References

ASCE Task Committee on Finite Element Analysis of Reinforced Concrete Structures, (1982), *Finite Element Analysis of Reinforced Concrete,* American Society of Civil Engineers, New York, NY.

ASCE-ACI Committee 447 (1993), *Finite Element Analysis of Reinforced Concrete II, (Proceedings of the International Workshop),* American Society of Civil Engineers, New York.

Belarbi, A. and Hsu, T.T.C. (1994), "Constitutive laws of concrete in tension and reinforcing bars stiffened by concrete", *Structural Journal of the American Concrete Institute,* **91**(4), 465-474.

Belarbi, A. and Hsu, T.T.C. (1995), "Constitutive laws of softened concrete in biaxial tension-compression", *Structural Journal of the American Concrete Institute,* **92**(5), 562-573.

Garza, G. (1996), "High strength concrete membrane elements reinforced with 2-D steel bars and 3-D welded wire grids", M. S. Thesis, Dept. of Civil and Environmental Engineering, University of Houston, Houston, TX.

Hsu, T.T.C. (1988), "Softened truss model theory for shear and torsion", *Structural Journal of the American Concrete Institute,* **85**(6), 624-635.

Hsu, T.T.C. (1993), *Unified Theory of Reinforced Concrete,* CRC Press, Inc., Boca Raton, FL.

Hsu, T.T.C., (1996). "Toward a unified nomenclature for reinforced concrete theory", *Journal of Structural Engineering, ASCE,* **122**(3), 275-283.

Hsu, T.T.C. and Zhang, L.X. (1996), "Tension stiffening in reinforced concrete membrane elements", *Structural Journal of the American Concrete Institute,* **93**(1), 108-115.

Hsu, T.T.C., Belarbi, A. and Pang, X.B. (1995), "A universal panel tester", *Journal of Testing and Evaluations, ASTM,* **23**(1), 41-49.

Hsu, T.T.C., Zhang, L.X. and Gomez, T. (1995), "A servo-control system for universal panel tester", *Journal of Testing and Evaluations, ASTM,* **23**(6), 424-430.

Hsu, T.T.C. and Zhang, L.X., (1997). "Nonlinear analysis of membrane elements by fixed-angle softened-truss model", *Structural Journal of the American Concrete Institute,* **94**(5), (Accepted for publication).

Pang, X.B. and Hsu, T.T.C. (1995), "Behavior of reinforced concrete membrane elements in shear", *Structural Journal of the American Concrete Institute,* **92**(6), 665-679.

Pang, X.B. and Hsu, T.T.C. (1996), "Fixed-angle softened-truss model for reinforced concrete", *Structural Journal of the American Concrete Institute,* **93**(2), 197-207.

Vecchio, F.J. and DeRoo, A. (1995). "Smeared crack modeling of concrete tension splitting", *Journal of Engineering Mechanics, ASCE,* **121**(6), 702-708.

Zhang, L.X. (1992), "Constitutive laws of reinforced elements with medium-high strength concrete", M. S. Thesis, Department of Civil and Environmental Engineering, University of Houston, Houston, TX.

Zhang, L.X. (1995), "Constitutive laws of reinforced elements with high strength concrete", Ph.D. Dissertation, Department of Civil and Environmental Engineering, University of Houston, Houston, TX.